

Diffractive Optical Element for Noise-reduced Beam Shaping of Multi-array Point Light Source

Jonghyun Lee¹, Joonku Hahn², and Hwi Kim^{1*}

¹Department of Electronics and Information Engineering,
Korea University Sejong Campus, Sejong 30019, Korea

²School of Electronic and Electrical Engineering, Kyungpook National University, Daegu 41566, Korea

(Received June 25, 2021 : revised August 4, 2021 : accepted August 10, 2021)

An arrayed diffractive optical element design for the beam-shaping of a multi-array light source is proposed. This is an essential device for recent optical security and face recognition applications. In practice, we devise a DC noise reduction technique featuring high fabrication error tolerance regarding the multi-array light source diffractive optical elements, as a necessary part of the proposed design method. The spherical diverging illumination leads to DC-conjugate noise spreading. The main idea is tested experimentally, and the multi-array light source diffraction pattern is investigated numerically.

Keywords : Diffractive optical element, Incoherent beam shaping, Noise management

OCIS codes : (050.1970) Diffractive Optics; (090.1995) Digital holography; (090.2870) Holographic display; (110.1758) Computational Imaging

I. INTRODUCTION

Recently, the diffractive optical element (DOE) has attracted unprecedented interest due to new emerging diffractive optic applications [1, 2]. With recent advances in nano-fabrication technology [3], the industrial opportunities for DOE are rapidly expanding. Some of the emerging fields adopting diffractive optics are near-eye displays for augmented reality (AR), optical security, and bio-optic sensors [4, 5]. Diffractive beam shaping using DOE in light detection and ranging (LiDAR) systems is considered a key part of next-generation electric and auto-vehicle industry technology. However, the inherent noise generation problem of DOEs, such as DC noise and conjugate noise, are still unresolved and remain a challenging issue for classical DOEs [6]. The generation of DC noise is a particularly notorious issue for general diffractive optics applications because DC generation is vulnerable to DOE fabrication error [7], leading to phase errors of the transmittance function. DC noise can be generated by the wavelength mismatch of broadband light source. Noise control is very important for the fields

such as material processing that require a low level of noise and beam uniformity [8–10]. In this paper, we propose a practical approach to reducing the average noise level by spreading DC and conjugate noise with high tolerance with respect to transmittance function error. Additionally, we will apply the design method to the design of a DOE for a multi-array light source.

II. METHODS AND RESULTS

To address the DC noise problem, we first present the conventional binary DOE with two phase levels, 0 and π , and its experimental observation (See Fig. 1). The schematic of the experimental setup and the binary DOE sample are shown in Figs. 1(a) and 1(b), respectively. A collimated laser beam of 650 nm wavelength illuminates the back of the DOE, and its diffraction intensity distribution is measured on the image plane. The continuous phase DOE profile is designed by the iterative Fourier transform algorithm (IFTA), and the binary phase of the DOE is approximated [11–13]. The fabricated DOE has a 1 μm pixel pitch, 4001

*Corresponding author: hwikim@korea.ac.kr, ORCID 0000-0002-4283-8982

Color versions of one or more of the figures in this paper are available online.



This is an Open Access article distributed under the terms of the Creative Commons Attribution Non-Commercial License (<http://creativecommons.org/licenses/by-nc/4.0/>) which permits unrestricted non-commercial use, distribution, and reproduction in any medium, provided the original work is properly cited.

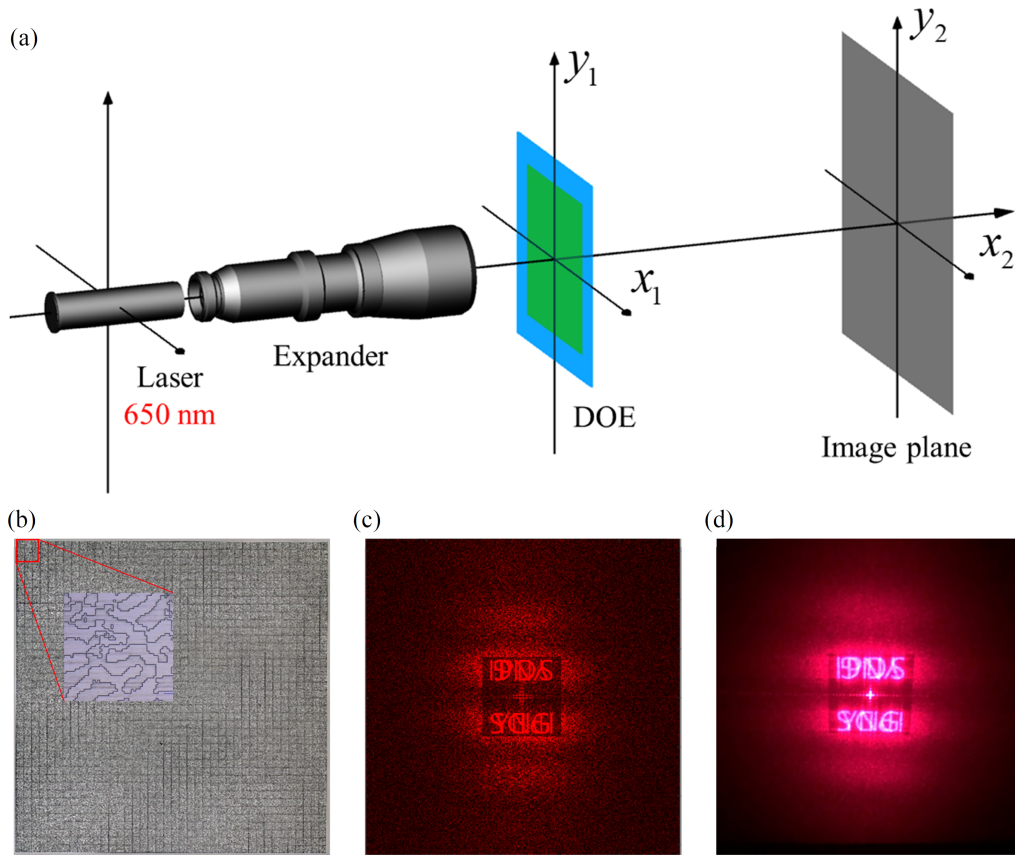


FIG. 1. Diffraction pattern of a conventional binary diffractive optical element (DOE): (a) experimental setup, (b) fabricated binary phase DOE with $1 \mu\text{m}$ pixel pitch, 4001×4001 resolution, and $4 \text{ mm} \times 4 \text{ mm}$ sample size, (c) numerical simulation result of the diffraction pattern, and (d) experimental observation of the diffraction pattern.

$\times 4001$ resolution, and $4 \text{ mm} \times 4 \text{ mm}$ footprint. Figures 1(c) and 1(d) present numerical simulation results of the diffraction intensity distribution in the image plane and its experimental observation, respectively, where the DC spot and conjugate image are observed. The simulation and experimental results are in precise agreement.

Since zero-th order DC noise and conjugate noise are inevitably generated in the binary phase or amplitude DOEs [14], extra noise filtering systems are popularly employed in many practical DOE system designs [15, 16]. Also, a removal of DC noise is a very important issue even in holographic displays such as head-up displays, and research progresses on methods for filtering [15] or spreading DC [17] in liquid crystal on silicon (LCoS) spatial light modulator (SLM) have been published. However, since miniaturization is a unique benefit of diffractive optics, such extra bulky filtering systems or devices are not acceptable for practical diffractive optics applications.

We address an indirect way to effectively reduce the average noise level of DC and conjugate noise. The central concept of the phase DOE design, which features a reduced average noise level is that the DC noise spreads as low as possible while the target diffraction image is separately maintained. Figure 2(a) presents a schematic of the pro-

posed approach. The two essential elements of the proposed scheme shown in Fig. 2(a) are the diverging incident light and the binary DOE multiplied by the convex lens phase profile.

As seen in Fig. 2(a), the diverging point light source illuminates the transmission-type DOE (x_1y_1 plane). In this case, the DC signal is still diverging because the DC component is neither influenced nor controllable by the DOE. The diverging light field coming out of a point source at the DOE plane is represented by

$$W(x_1, y_1) = e^{\frac{j\pi}{\lambda F}(x_1^2 + y_1^2)}, \quad (1)$$

where λ and F are the wavelength and the distance of the point source from the DOE plane, respectively.

The transmittance function of the DOE $t(x_1, y_1)$ is assumed to have two modulating terms, which consist of $\bar{t}(x_1, y_1)$ in the case of the target signal and $\bar{t}^*(x_1, y_1)$ in the case of the conjugate noise, and a non-modulated constant DC term as follows:

$$t(x_1, y_1) = \bar{t}(x_1, y_1) + \bar{t}^*(x_1, y_1) + DC. \quad (2)$$

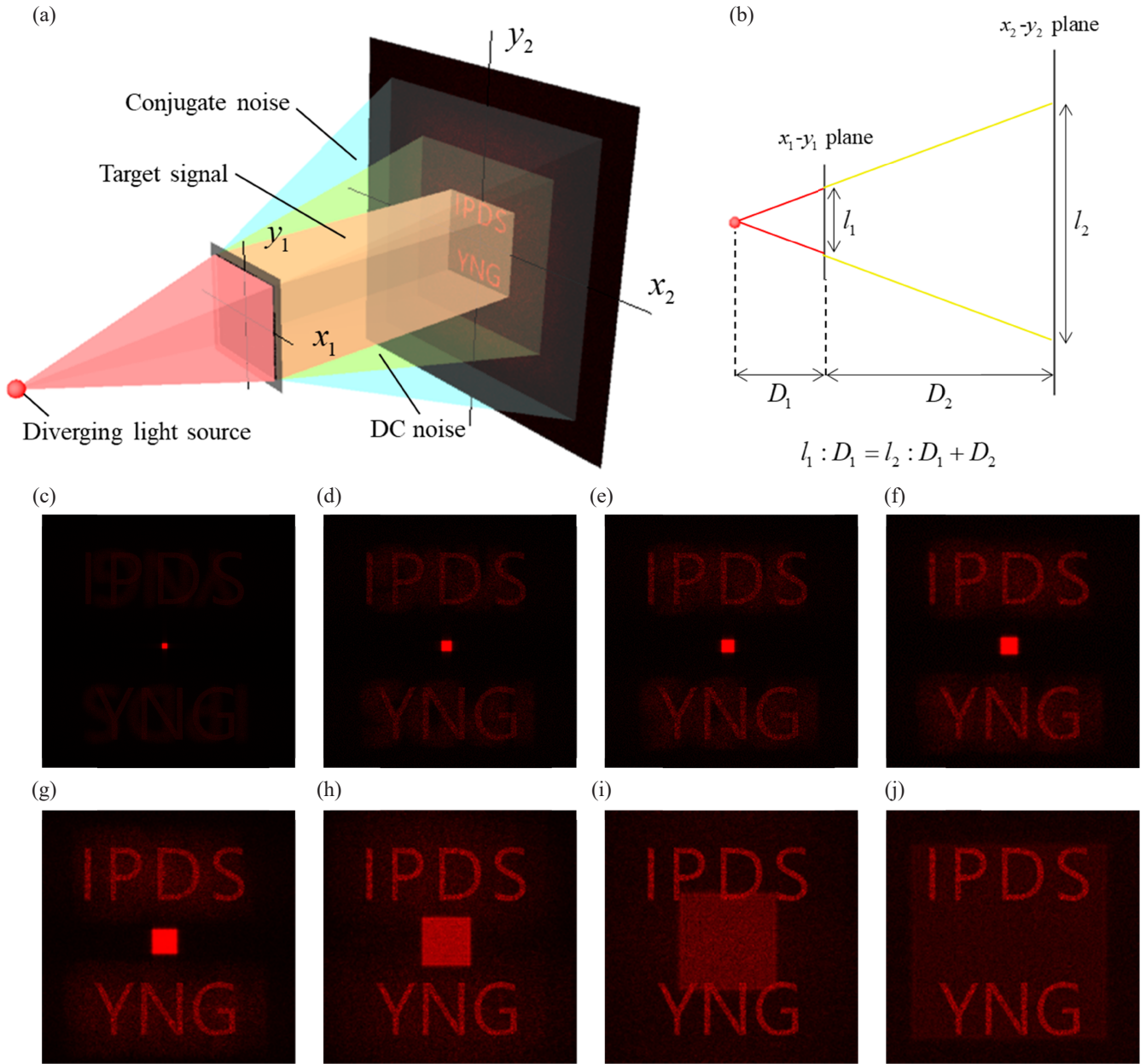


FIG. 2. The system scheme and noise spreading simulation results for a single diverging illumination source. (a) Operation schematic diagram of the proposed DOE system, (b) the design condition of a light source, DOE size l_1 , and the zeroth diffraction zone l_2 , and numerical simulations of the DC noise spreading in the diffraction pattern for focal lengths of (c) 1 m, (d) 0.5 m, (e) 0.4 m, (f) 0.3 m, (g) 0.2 m, (h) 0.1 m, (i) 0.05 m, and (j) 0.025 m.

The complex field distribution of the DOE under the illumination $W(x_1, y_1)$ is obtained as

$$U(x_1, y_1) = t(x_1, y_1)W(x_1, y_1). \quad (3)$$

The DOE is designed to include the convex phase profile that is enabled to compensate for the diverging phase component of the incoming wave-field and diffract to form a designed intensity distribution in the image plane. The DC and conjugate noise terms are spread over the image plane. The modulating term $\bar{t}(x_1, y_1)$ is formed by the multiplica-

tion of the CGH pattern generating the target diffraction pattern and the convex phase function, and this cancels the diverging spherical phase of the incidence field $W(x_1, y_1)$. The modulating term $\bar{t}(x_1, y_1)$ excluding the conjugate term is designed as

$$\bar{t}(x_1, y_1) = t_{\text{DOE}}(x_1, y_1) e^{-\frac{j\pi}{\lambda F}(x_1^2 + y_1^2)}, \quad (4)$$

where $t_{\text{DOE}}(x_1, y_1)$ represents the phase function for reconstructing a target signal. By substituting Eq. (4) into Eq. (3),

we find the complex field distribution $U(x_1, y_1)$ on the DOE plane as

$$U(x_1, y_1) = t_{\text{DOE}}(x_1, y_1) + t_{\text{DOE}}^*(x_1, y_1) e^{\frac{j2\pi}{\lambda F}(x_1^2 + y_1^2)} + \text{DC} \cdot e^{\frac{j\pi}{\lambda F}(x_1^2 + y_1^2)}. \quad (5)$$

The transform of the forward propagation is referred to the Fresnel transform [16] from the DOE plane (x_1, y_1 plane) to the image plane (x_2, y_2 plane), and the Fresnel transform $\text{FrT}\{f(x_1, y_1); z\}$ of the function $f(x_1, y_1)$ is defined by

$$\text{FrT}\{f(x_1, y_1); z\} = \int_{-\infty}^{\infty} \int_{-\infty}^{\infty} f(x_1, y_1) e^{\frac{j\pi}{\lambda z}[(x_2 - x_1)^2 + (y_2 - y_1)^2]} dx_1 dy_1, \quad (6)$$

where z and λ denote the propagation distance and wavelength of the incident wave, respectively. Accordingly, the diffraction image $F(x_2, y_2)$ on the image plane is represented by

$$F(x_2, y_2) = \text{FrT}\{U(x_1, y_1); z\}. \quad (7)$$

As the conjugate term $t_{\text{DOE}}^*(x_1, y_1)$ and the DC term diverge due to the spherical carrier wave, the spreading of DC and conjugate noise on the image plane is expected.

Conventional phase quantization is used to multi-step phase-only DOE. The diverging light field can be realized by setting up a concave lens with the same focal length as the convex lens phase profile applied to the DOE. If the divergent light generated by the concave lens is incident onto the proposed DOE with the corresponding convex lens phase profile, the spherical phase profile of the incidence field is canceled out and the target signal is reconstructed correctly in the region of interest (ROI), since the phase profiles of two lens profiles cancel each other out. The diffraction image at the image plane is obtained by the Fresnel diffraction transform.

The phase function of the transmittance function $\bar{t}(x, y)$ is fabricated. In this scheme, the designed transmittance $t_{\text{DOE}}(x, y)$ carries out diffraction pattern generation, while the conjugate noise as well as the non-controllable DC term spread broadly over the image plane (x_2, y_2 plane), as shown in Fig. 2. The divergence angle of DC and the corresponding coverage areas can be controlled by the distance parameter F in Eq. (5).

The optimized position of a light source can be calculated as shown in Fig. 2(b). As the DOE can compensate the phase of the diverging light source, the position of the light source should be optimized to cover the zero-th region. The optimized position of a light source is represented to

$$D_1 = \frac{l_1}{l_2 - l_1} D_2, \quad (8)$$

where parameters are the optimized position D_1 of a light

source, the propagation distance D_2 , the size l_1 of DOE, and the size l_2 of zero-th region. By the Fresnel diffraction, the size of zero-th region is $l_2 = \lambda D_2 / p$, where p is the pixel pitch of DOE. If the position of a light source is too short, compensation for the diverging light source will not be done properly. Accordingly, it should be optimized by calculating the appropriate position.

The binary phase DOE is designed according to the above mentioned process and the simulated results for the focal lengths of 1 m, 0.5 m, 0.4 m, 0.3 m, 0.2 m, 0.1 m, 0.05 m, and 0.025 m are presented in Figs. 2(c)–2(j), respectively. Regardless of the distance parameter F and the DC noise coverage, the target diffraction image ‘IPDS YNG’ is clearly observed in the image plane.

The verification experiment was undertaken. The binary DOE for the same target image as in Fig. 1 was fabricated [Fig. 3(b)] and tested in the experimental setup depicted in Fig. 3(a). A collimated beam is transformed into a diverging field through a concave lens of 2.5 cm focal length.

The DC reduction-binary type DOE sample in Fig. 3(b) has 1 μm pixel pitch, 4001 \times 4001 resolution, and 4 mm \times 4 mm footprint. The numerical simulation and the experimental observation results of the diffraction image are compared in Figs. 3(c) and 3(d), respectively. The diffraction image for the target signal, ‘IPDS YNG’, is observed in ROI. In contrast to the results in Figs. 1(c) and 1(d), the reconstructed image has low-level noise and high image quality.

In recent industrial applications, multi-array light sources such as vertical-cavity surface-emitting laser (VCSEL) and light-emitting diode (LED) arrays are popular in the diffractive optic system. The representative example of the multi-light source diffractive system is the LiDAR module installed in electric and auto vehicles. In order to project beam array on the free space, the DOE used in those fields is used as a function of splitting beam. In this paper, we design and analyze the DC reduction-binary beam shaping DOE for an incoherent point source array. In Fig. 4, the DOEs for 3 \times 3 arrayed light source are designed with and without DC reduction function and they are compared to each other in terms of the quality of far-field diffraction intensity distribution. The point source wavelength is 650 nm and assumed to be located 1.25 mm from the DOE as seen in Fig. 4(a).

The distance between adjacent light sources is about 0.9 mm. The proposed multilevel DOE sample in Fig. 4(b) is designed with a 1 μm pixel pitch, 3,333 \times 3,333 resolution, and 3.3 mm \times 3.3 mm footprint. Figures 4(c) and 4(d) show each image reconstructed with DC noise and the reduction diverging DC noise in the ROI. Despite using a multi-array incoherent light source, a clear target signal can be observed due to diverging the DC noise over the whole region.

In the case of using the multi-array diverging light source, each source is represented by

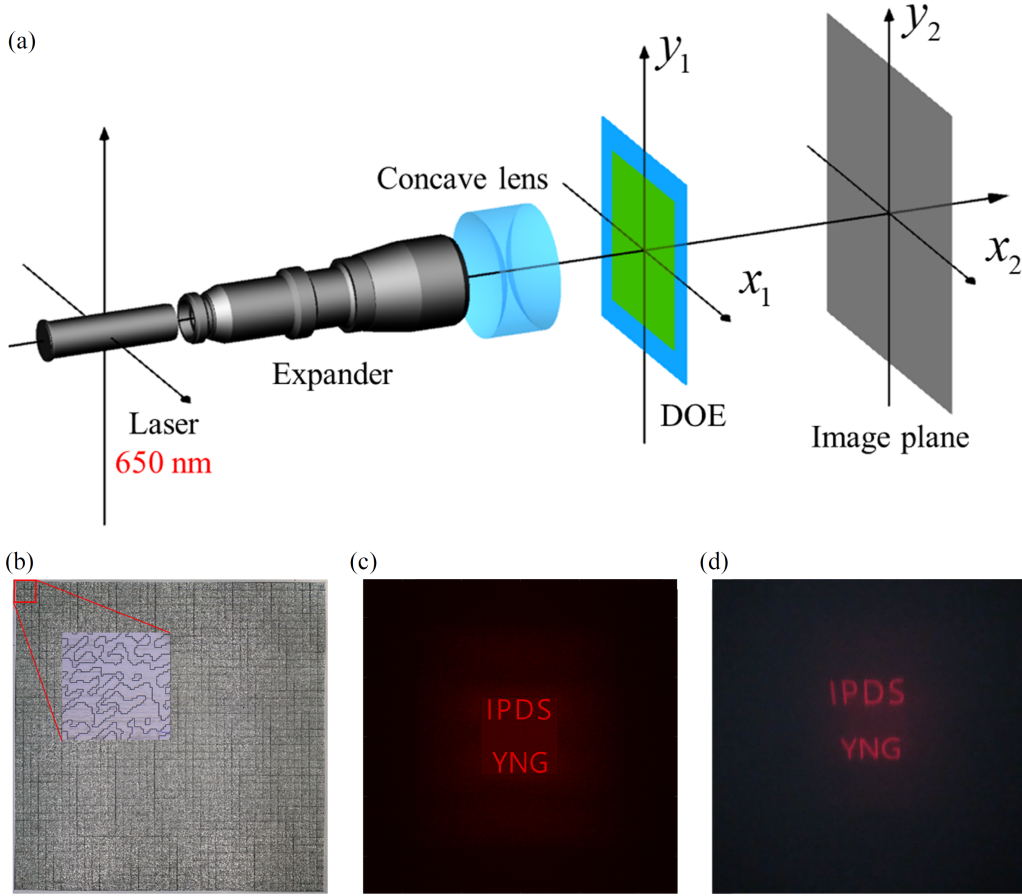


FIG. 3. Diffraction pattern of the proposed binary DOE: (a) experimental setup, (b) fabricated binary phase DOE with 1 μm pixel pitch, $4,001 \times 4,001$ resolution, and $4 \text{ mm} \times 4 \text{ mm}$ sample size, (c) numerical simulation result of the diffraction pattern, and (d) experimental observation of the diffraction pattern.

$$W_p(x_1, y_1) = e^{\frac{j\pi}{\lambda F} \left((x_1 - d_{p,x})^2 + (y_1 - d_{p,y})^2 \right)}, \quad (9)$$

where $d_{p,x}$ and $d_{p,y}$ are the shifted x-position and shifted y-position of each light source on the source plane and p is the source index. Here, we assume that the point sources are incoherent with respect to each other.

The p th transmittance function of the DOE for the shifted single light source $W_p(x_1, y_1)$ is represented as

$$t_p(x_1, y_1) = \bar{t}_p(x_1, y_1) + \bar{t}_p^*(x_1, y_1) + DC_p. \quad (10)$$

The modulating term $\bar{t}_p(x_1, y_1)$ is designed to be

$$\bar{t}_p(x_1, y_1) = t_{\text{DOE}}(x_1, y_1) e^{-\frac{j\pi}{\lambda F} \left((x_1 - d_{p,x})^2 + (y_1 - d_{p,y})^2 \right)}, \quad (11)$$

where $t_{\text{DOE}}(x_1, y_1)$ represents the designed phase function forming the target image and is commonly applied for every point light sources.

We set the total transmittance function of the DOE, $t(x_1, y_1)$, according to

$$t(x_1, y_1) = \sum_{p=1}^N t_p(x_1, y_1). \quad (12)$$

The complex field distribution formed by the total DOE $t(x_1, y_1)$ illuminated by the p th single diverging light source $W_p(x_1, y_1)$ is obtained as

$$U_p(x_1, y_1) = t(x_1, y_1) W_p(x_1, y_1). \quad (13)$$

The total field intensity distribution on the image plane seen in Fig. 4(d) illuminated by all point light sources is represented by the incoherent superposition form:

$$I_{\text{total}}(x_2, y_2) = \sum_{p=1}^N \left| \text{FrT} \{ U_p(x_1, y_1); z \} \right|^2. \quad (14)$$

Each individual light source comprising the multi-array light source is designed to illuminate its own corresponding DOE without interfering with the other DOEs, since the cross-interference can degrade the diffraction image. Figure 5 shows a comparison of the diffraction intensity distributions with respect to the source illumination overlap area. It is apparent that the diffraction intensity distribution with

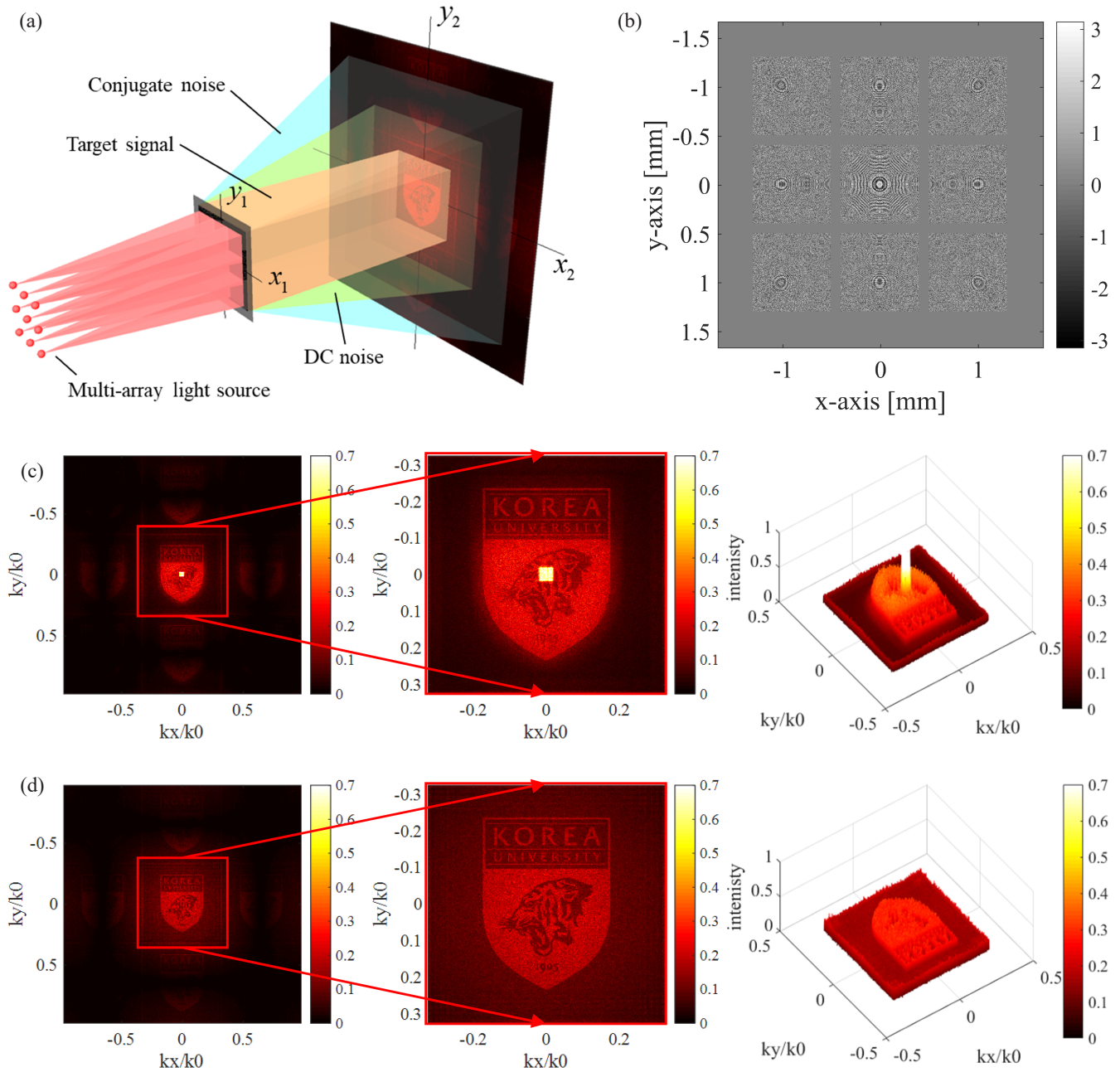


FIG. 4. The system scheme and noise spreading simulation results for multi-array diverging illumination source. (a) Operation schematic diagram of the proposed DC reduction of DOE for the multi-array light source, (b) the proposed 3×3 multi-arrayed phase DOE profile $t_{\text{DOE}}(x_1, y_1)$ with DC-conjugate noise spreading. Comparison of (c) the diffraction pattern of the conventional DOE with strong DC spot and (d) that of the proposed DOE with DC-conjugate spreading.

no-overlap area in Fig. 5(a) has the superior diffraction efficiency, 47.71%. As the illumination overlap increases, the diffraction image quality becomes increasingly degraded even though the DC spot is spread over the image plane. The proposed method of DC spreading is neither real DC noise rejection nor filtering. DC noise rejection without additional bulky filtering systems is difficult to achieve. In the recent security application, the dot-array pattern is generated by the DOE. In this application, the binary thresholding is applied to the dot-array diffraction pattern. The strong

DC spot needs to be spread for this type of application.

III. CONCLUSION

In conclusion, we proposed the design of an arrayed phase-type DOE for an incoherent multi-array point light source with a DC-conjugate noise spreading property. Also, through simulation and experiment results, we presented that, instead of simply magnifying the reconstructed projection image, the phase of the target signal wave is

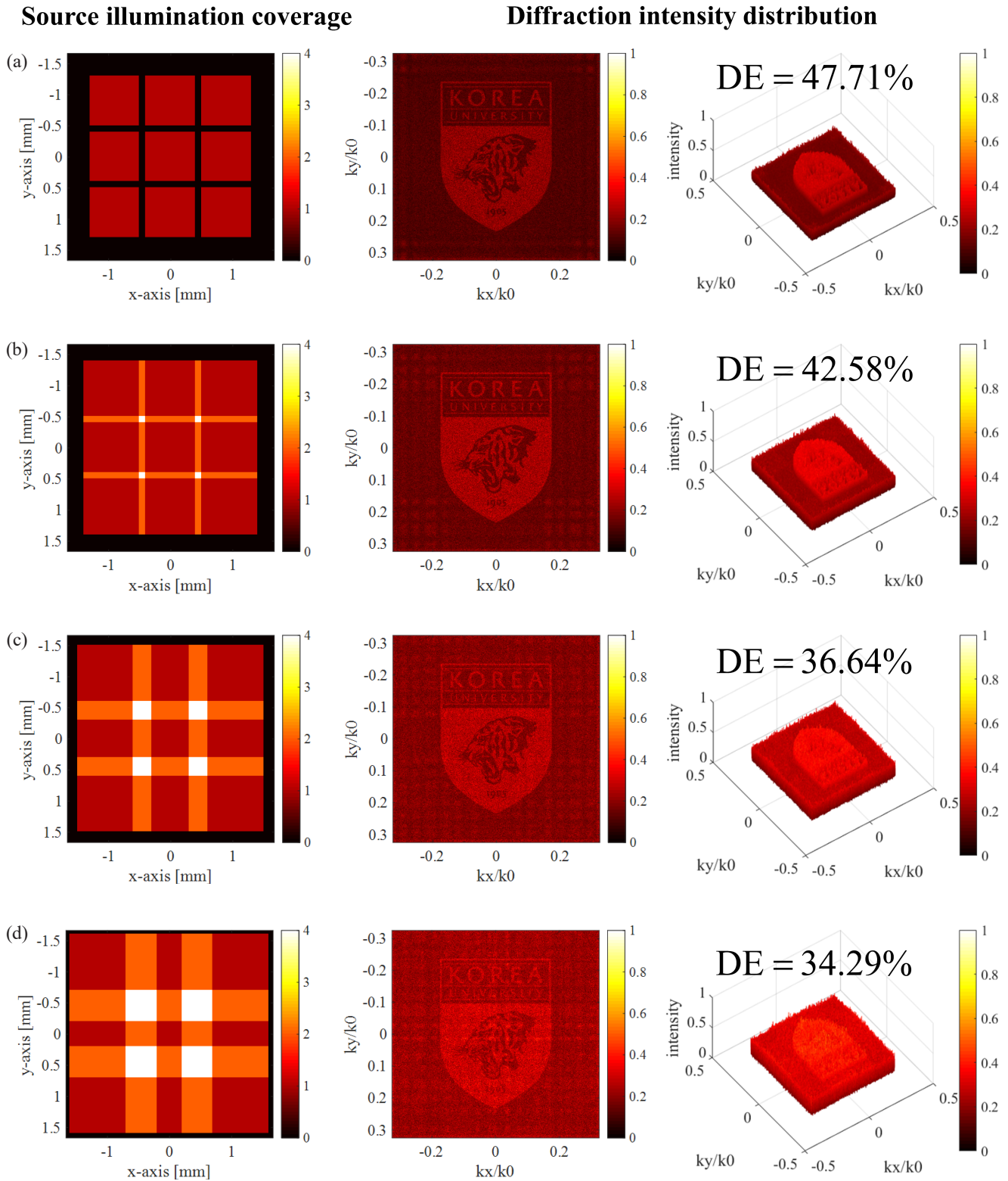


FIG. 5. Comparative analysis of the total intensity distribution and diffraction efficiency (DE) with respect to the source illumination overlap area. The overlap of each single-source area is (a) non-overlap (0%), (b) 10%, (c) 25%, and (d) 35%, respectively. The left column shows the source illumination coverage highlighting the illumination overlap area. The central and right columns present the numerical simulation results of the diffraction intensity distribution for each case, and the resulting diffraction efficiency.

maintained and the quality of the reconstructed image is improved by spreading the DC and conjugate wave by the divergent spherical phase. Especially, it is superior for use in the variety of fields in that it can be applied not only for a single source but also for multi-array source. Further optimization can be performed using other nonlinear optimization algorithm such as stochastic gradient descent (SGD), nonlinear conjugate gradient method rather than IFTA. We will deal with this topic in our next research. The flexibility of using DC-conjugate noise spreading supports the practical application of DOEs, such as to LiDAR techniques, facial recognition, and vision camera for autonomous driving.

ACKNOWLEDGMENT

This study was supported by National Research Foundation of Korea (NRF) (NRF-2019R1A2C1010243).

REFERENCES

1. J. Hong, Y. Kim, H.-J. Choi, J. Hahn, J.-H. Park, H. Kim, S.-W. Min, N. Chen, and B. Lee, "Three-dimensional display technologies of recent interest: principles, status, and issues," *Appl. Opt.* **50**, H87–H115 (2011).
2. S. V. Karpeev, V. V. Podlipnov, S. N. Khonina, V. D. Parandin, and K. N. Tukmakov, "Anisotropic diffractive optical element for generating hybrid-polarized beams," *Opt. Eng.* **58**, 082402 (2018).
3. S. H. Hwang, J. Cho, S. Jeon, H.-J. Kang, Z.-J. Zhao, S. Park, Y. Lee, J. Lee, M. Kim, J. Hahn, B. Lee, J. H. Jeong, H. Kim, and J. R. Youn, "Gold-nanocluster-assisted nanotransfer printing method for metasurface hologram fabrication," *Sci. Rep.* **9**, 3051 (2019).
4. L. Mi, C. P. Chen, Y. Lu, W. Zhang, J. Chen, and N. Maitlo, "Design of lensless retinal scanning display with diffractive optical element," *Opt. Express* **27**, 20493–20507 (2019).
5. K. T. P. Lim, H. Liu, Y. Liu, and J. K. W. Yang, "Holographic colour prints for enhanced optical security by combined phase and amplitude control," *Nat. Commun.* **10**, 25 (2019).
6. P. Bhuvaneshwari and A. B. Therese, "Hybrid algorithm for twin image removal in optical scanning holography," *Int. J. Comput. Aided Eng. Technol.* **12**, 33–54 (2020).
7. A. G. Poleshchuk, "Fabrication of phase structures with continuous and multilevel profile for diffraction optics," *Proc. SPIE* **1574** (1991).
8. M. Duocastella and C. B. Arnold, "Bessel and annular beams for materials processing," *Laser Photonics Rev.* **6**, 607–621 (2012).
9. S. Katz, N. Kaplan, and I. Grossinger, "Using diffractive optical elements: DOEs for beam shaping—fundamentals and applications," *Optik & Photonik* **13**, 83–86 (2018).
10. S. Katz, "Diffractive optical elements: minimizing zero order," (Photonics spectra, Published date: February 2018), <https://www.photonics.com/Article.aspx?AID=62935&PID=5&VID=149&IID=986> (Accessed date: March 2018).
11. F. Wyrowski, "Diffractive optical elements: iterative calculation of quantized blazed phase structure," *J. Opt. Soc. Am. A* **7**, 961–969 (1990).
12. H. Kim and B. Lee, "Optimal non-monotonic convergence of iterative Fourier transform algorithm," *Opt. Lett.* **30**, 296–298 (2005).
13. H. Kim, B. Yang, and B. Lee, "Iterative Fourier transform algorithm with regularization for the optimal design of diffractive optical elements," *J. Opt. Soc. Am. A* **21**, 2353–2365 (2004).
14. E. Cuche, P. Marquet, and C. Depeursinge, "Spatial filtering for zero-order and twin-image elimination in digital off-axis holography," *Appl. Opt.* **39**, 4070–4075 (2000).
15. J. Cho, S. Kim, S.-W. Park, B. Lee, and H. Kim, "DC-free on-axis holographic display using a phase-only spatial light modulator," *Opt. Lett.* **43**, 3397–3400 (2018).
16. J. Roh, K. Kim, E. Moon, S. Kim, B. Yang, J. Hahn, and H. Kim, "Full-color holographic projection display system featuring an achromatic Fourier filter," *Opt. Express* **25**, 14774–14782 (2017).
17. J. Skirnewskaja, Y. Montelongo, P. Wilkes, and T. D. Wilkinson, "LiDAR-derived digital holograms for automotive head-up displays," *Opt. Express* **29**, 13681–13695 (2021).